Intracellular pH Regulation: Characterization and Functional Investigation of H+ Transporters in *Stylophora Pistillata*

Laura Capasso
Centre Scientifique de Monaco
Philippe Ganot
Centre Scientifique de Monaco
Víctor Planas-Bielsa
Centre Scientifique de Monaco
Sylvie Tambutté
Centre Scientifique de Monaco
Didier Zoccola (zoccola@centrescientifique.mc)
Centre Scientifique de Monaco https://orcid.org/0000-0002-1524-8098

Research article

Keywords: H+ transport, reef-building corals, pH regulation, gene expression, ocean acidification

Posted Date: November 2nd, 2020

DOI: https://doi.org/10.21203/rs.3.rs-98613/v1

Version of Record: A version of this preprint was published at BMC Molecular and Cell Biology on March 8th, 2021. See the published version at https://doi.org/10.1186/s12860-021-00353-x.

Abstract

Background: Reef-building corals regularly experience changes in intra and extracellular H^+ concentration ($[H^+]$) due to physiological and environmental processes. Stringent control of $[H^+]$ is required for the maintenance of homeostatic acid-base balance in coral cells and is achieved through the regulation of intracellular pH (pH_i). This task is especially challenging for reef-building corals that share an endosymbiotic relationship with photosynthetic dinoflagellates (family Symbiodinaceae), which exert a significant effect on the pH_i of coral cells. Despite their importance, the pH regulatory proteins involved in the homeostatic acid-base balance have been scarcely investigated in corals. Here, we reported the full characterisation in terms of genomic structure, domain topology and phylogeny of three majors H^+ transporter families implicated in pH_i regulation; we investigated their tissue-specific expression and we assessed the effect of seawater acidification on their level of expression.

Results: We identified members of the Na^+/H^+ exchanger (SLC9), vacuolar-type electrogenic H^+-ATP hydrolases (V-ATPase) and voltage-gated proton channels (H_vCN) families in the genome and transcriptome of *S. pistillata*. In addition, we identified a novel member of the H_vCN gene family in the cnidarian subclass Hexacorallia, which has never been described in any species to date. We also reported key residues that participate to the H^+ transporters substrate specificity, protein function and regulation. Lastly, we demonstrated that some of these have different tissue expression patterns and are mostly unaffected by exposure to seawater acidification.

Conclusions: In this study, we provide the first characterization of the H^+ transporters genes that contribute to homeostatic acid-base balance in coral cells. This work will enrich knowledge about basic aspects of coral biology, bearing important implications for our understanding of how corals regulate their intracellular environment.

1. Background

Coral reefs are among the most valuable ecosystems on earth, harbouring more than one-third of the oceans' biodiversity and providing economic benefits to tropical coastal nations worldwide [1]. Scleractinian corals are the major constructors of coral reefs and most of them have mutualistic relationships with endosymbiotic dinoflagellates (family Symbiodinaceae) -symbiotic corals-, which provide photosynthetic products for support of coral metabolism, growth and reproduction [2–4]. Despite their environmental significance, scleractinian corals face many challenges to their survival, including ocean acidification (OA), as a result of rising carbon dioxide levels in the atmosphere [5]. Effects of OA on coral calcification rate and skeletal growth have been previously documented [6–9], with varied species-specific responses. Most of these effects have been proposed to be linked to acid-base regulatory processes, leading to altered ionic concentration, energy expenditure and allocation [10]. Although acid-base regulatory processes might modulate physiological responses to OA, the pH regulatory proteins responsible for acid-base homeostasis are still poorly characterized in corals.

Corals are dipoblastic animals, meaning they are made of two cell layers, an ectoderm and an endoderm, separated by a layer of mesoglea. Both ectoderm and endoderm are present in the oral and aboral tissue, which lie either side of the gastrovascular cavity (coelenteron) [11]. Each tissue possesses several cell subtypes that achieve acid-base homeostasis through pH regulation within physiological boundaries compatible with cell functioning [12]. This is especially challenging for symbiotic corals, as photosynthesis has a significant effect on the pH of coral cells [13, 14]. Symbiotic corals can experience large variation of extracellular pH (pH_e), under physiological (e.g. respiration, calcification and photosynthesis) and environmental (e.g. metabolism of reef-associated organisms, tides, water flow, upwelling and ocean acidification) parameters. For example, day-symbiont photosynthesis and night-time respiration, of both host and symbiont, drive wide pH_e variations (from pH 8.5 to 6) in the internal fluids of the coelenteron [13–18]; or, exposure to acidified seawater decreases the pH_e in the extracellular calcifying medium (ECM) [9], where calcification occurs. These pH_e variations can also have an impact on the regulation of intracellular pH (pH_i). For example, decreases in the pH_e of the ECM (from 8.3 to 7.8), under acidified seawater, affect the pH_i of the calicoblastic cells. Despite these variations, coral cells are able to maintain their pH_i within narrow limits (7.1–7.4) [9], showing that corals possess efficient pH_i regulatory mechanisms that account for this stability.

Under pH_i challenges, an appropriate response depends on the ability to sense acid-base disturbances and react through acid-base transporting mechanisms [19]. Over the previous years, a number of acid-base cellular sensors and transport proteins have been proposed in corals on the basis of those characterized in vertebrates [20–22]. Acid-base transport proteins, in charge of pH_i regulation, fall into two groups: HCO_3^- (solute carrier-SLC transporter family 4 and 26) and H^+ membrane transporters [23]. Based on the energy source provided for H^+ extrusion, H^+ membrane transporters can be further divided in: transporters, pumps and channels. Transporters can move H^+ against their electrochemical gradient by coupling H^+ transport with pre-existing ion gradients as energy source. This group includes the SLC9 family, also known as Na^+/H^+ exchanger, which harness the electrochemical gradient of Na^+ maintained by the Na^+/K^+-ATPase [24]. The SLC9 family can be further divided into three subfamilies: subfamily A 1–9 (cation proton antiporter 1-CPA1), subfamily B 1–2 (cation proton antiporter 2-CPA2) and subfamily C 1–2 (Na-transporting carboxylic acid decarboxylase, NaT-DC) [25]. The second group of H^+ membrane transporters in charge of pH_i regulation include H^+ pumps, which allow H^+ to move against their concentration gradient by coupling H^+ transport to ATP hydrolysis. The vacuolar-type electrogenic H^+-ATP hydrolases (V-ATPases), which transports H^+ via the V_0 V-ATPase subunit-a [26], and the plasma-membrane Ca^{+2}-ATPase (PMCA), which extrudes Ca^{+2} in exchange of H^+ [19, 27, 28], belong to this group. Although some studies claim that pH_i regulation is not the primary role of these H^+ pumps in most mammalian cells (Reviewed in Casey et al., 2010), others have suggested the opposite [29–32]. The last group, H^+ channels, allows H^+ to passively diffuse down their electrochemical gradient whenever the regulatory gate is open and include voltage-gated proton channels (H_vCN) [33, 34].

Despite their fundamental importance in pH_i regulation, the molecular characterization of these H^+ transporters is missing in Cnidaria. In corals, HCO_3^- transporters have been characterised [20] contrary to the H^+ membrane transporters for which information is limited to the Ca^{+2}-ATPase [35] and the V-ATPase V_1 V-ATPase subunit B [36]. In the present study, we provide a full characterisation in terms of genomic structure, domain topology and phylogeny of the principal H^+ transporters, involved in intracellular pH regulation and maintenance of cell physiological homeostasis, in the symbiotic coral *Stylophora pistillata*. These include: the Na^+/H^+ exchangers, which are ion transporters that concurrently transport Na^+ into the cell and H^+ out of the cell; voltage-gated H^+ channels (H_vCN), which represent a specific subset of proton channels that have voltage- and time-dependent gating in a way that they open only to extrude H^+ from the cell; and the V_0 V-ATPase subunit-a, which connects the two portions (V_0 and V_1) of the multi-subunit enzyme V-ATPase and is crucial for proton transport [19, 30, 37–39]. Furthermore, we characterize the gene expression patterns of H^+ transporters to determine whether they are differentially expressed in the coral tissues, and we discuss their potential physiological roles. In addition, we investigate the molecular response of *S. pistillata* to ocean acidification, by assessing the effect of external seawater acidification on the levels of H^+ transporter expression after one-week and one-year of exposure.

2. Results

2.1.1 Candidate Na^+-H^+ exchanger (SLC9) in *S. pistillata*: gene structure, amino acid sequence and phylogenetic analysis

We identified genes homologous to human *SLC9* in the genome and transcriptome of *S. pistillata* [40, 41]. Phylogenetic analysis of *S. pistillata* SLC9 proteins (spiSLC9) with functionally characterised SLC9 in human allowed us to group the corresponding *S. pistillata* genes within three subfamilies: A, B and C (Fig. 1). Members of Subfamily A are distributed in two different clusters (plasma membrane and organelle), which contain plasma membrane and organelle homologs. In addition, organelle homologs are on two distinct branches (A8 and A6/7). Of the seven *SLC9* genes identified in *S. pistillata*: four belong to subfamily A (NHE subfamily), one (*spiSLC9A1*) is a plasma membrane homolog, two (*spiSLC9A6* and *spiSLC9A7*) are A6/7 organelle homologs and one (*spiSLC9A8*) is a A8 organelle homolog; two (*spiSLC9B1* and *spiSLC9B2*) belong to subfamily B (NHA subfamily); and one (*spiSLC9C*) belongs to subfamily C (mammalian sperm NHE-like subfamily). Gene and transcript information of SLC9 family members are given in Additional Files 1 and 2.

The exchange domain of spiSLC9s is predicted to have 8 to 12 TMs (Additional File 3), which display sequence conservation in opposition to the higher variability observed at the N-terminus and C-terminus of the proteins. Sequence comparison of spiSLC9s showed similitude within members of the same subfamily and the percentage of similarity and identity vary for each subfamily. For members of subfamily A, the percentage of similarity varies between 50–57% (sharing 35% of identity). Whereas, members of subfamily B share 78% percentage of similarity (sharing 62% of identity). spiSLC9 proteins

exhibit also similitude with hSLC9: spiSLC9A have 42–55% identity, 60–71% of similarity to hSLC9A; spiSLC9B have 43–47% identity, 61–66% of similarity to hSLC9B and spiSLC9C has 26% identity, 50% of similarity to hSLC9C. In addition, spiSLC9s possess conserved features with hSLC9s, including: residues relevant for Na^+/H^+ exchanger activity, such as F161, P167-168, R440 and G455-456, for members of Subfamily A (Additional File 4); glycine zipper sequences (SLC9B1-GZ1: 275–283; SLC9B2-GZ1: 184–192; GZ2: 210–216; GZ3: 263–271), for members of Subfamily B (Additional File 5); a conserved voltage-sensing domain (VSD), composed of four transmembrane segments S1-S4, and a cyclic nucleotide-binding domain (CNBD) for the member of subfamily C (Additional File 6).

With regard to post-translational modifications: 24, 17, 14, 12, 7, 7 and 27 phosphorylation sites were predicted for spiSLC9A1, spiSLC9A6, spiSLC9A7, spiSLC9A8, spiSLC9B1, spiSLC9B2 and spiSLC9C respectively. 4 N-glycosylation sites were predicted for spiSLC9A1 (N33, N183, N332 and N586) and spiSLC9A6 (N108, N124, N349 and N370). Whereas 5, 3, 2, 1 and 4 N-glycosylation sites were predicted for spiSLC9A7 (N120, N133, N292, N364 and N385), spiSLC9A8 (N41, N48 and N147), spiSLC9B1 (N279 and N365), spiSLC9B2 (N293) and spiSLC9C (N340, N972, N1132 and N1155).

2.1.2 Candidate V_0 V-ATPase subunit-a in *S. pistillata*: gene structure, amino acid sequence and phylogenetic analysis

As previously performed with *spiSLC9*, we identified one gene homologous to human *V_0 V-ATPase subunit-a* in the genome and transcriptome of *S. pistillata*. Gene and transcript information of *V_0 V-ATPase subunit-a* gene are given in Fig. 2A and the Additional File 2. *spiV_0 V-ATPase subunit-a* exists in four splice variants and it is part of the 14 subunits composing the spiV-ATPase (Additional File 7).

spiV_0 V-ATPase subunit-a protein has six predicted TMs (Additional File 3) and exhibits similarity to human homologs (44–64% of similarity and 59–76% of identity). Several residues (Fig. 2B) are conserved between spiV_0 V-ATPase and hV_0 V-ATPase, such as: R735, L739, H743, E789, L746, R799 and V803. With regard to post-translational modifications, 13 phosphorylation sites (S7, T137, S195, T217, S223, T354, 7455, Y461, T522, S635, S689, S691, S706) and 2 N-glycosylation sites (N286 and N378) were predicted for spiV_0 V-ATPase subunit-a.

As previously done, we identified putative V_0 V-ATPase subunit-a homologs in other species (Fig. 3).

2.1.3 Candidate voltage-gated H^+ channels (H_vCN) in S. pistillata: gene structure, amino acid sequence and phylogenetic analysis

Data mining in the genome and transcriptome of *S. pistillata* allowed us to identify two genes, *spi$H_vCN1.1$* and *spi$H_vCN1.2$*, homologous to human *hH_vCN1*. Gene and transcript information of the two *spiH_vCN* genes are given in Fig. 4A and Additional File 2.

spiH_vCN1.1 and spiH_vCN1.2 share 35% of identity, 62% of similarity and possess four predicted transmembrane domains (TMs) (Additional File 3). TMs display sequence conservation (Fig. 4B), with highly conserved residues relevant for H_vCN activity mostly located in the TMs. The two spiH_vCNs

sequences exhibit similitude with hH_vCN1 ($spiH_vCN1.1$ has 40% identity, 67% of similarity to hH_vCN1 and $spiH_vCN1.2$ has 28% identity, 61% of similarity to hH_vCN1). Several basic and acidic residues (R205, R208, R211, H140, E153 and D174) are conserved between $spiH_vCNs$ and hH_vCN1. Whereas D112, D123, D185 and E119 are conserved only between $spiH_vCN1.1$ and hH_vCN1. With regard to post-translational modifications, phosphorylation sites were predicted for both proteins: S8, T22, Y76 and S162 for $spiH_vCN1.1$, and T10, T18, T28, S46, S121 and S144 for $spiH_vCN$ 1.2. Furthermore, N48 was predicted to be N-glycosylated in $spiH_vCN1.1$ while no N-glycosylation sites were predicted in $spiH_vCN1.2$.

Sequence similarity searches of available proteomic and genomic datasets using the human H_vCN1 protein identified putative H_vCN homologs in several evolutionary distant species (Fig. 5). Hexacorallia are the only species that compared to other animals possess two H_vCNs, which split the tree in two groups: $H_vCN1.1$ and $H_vCN1.2$.

2.2 Tissue-Specific Gene Expression of *S. pistillata* H^+ transporters

Quantitative real-time PCR was used to detect the H^+ transporters mRNA expression (relative mRNA quantification-R_q) in the oral fraction and total colony (prepared according to Ganot et al., 2015 and Zoccola et al., 2015) of *S. pistillata*. Results show no differential expression for *spiSLC9A1*, *B1, B2 and* $spiV_0$ *V-ATPase subunit-a* (Fig. 6A, -E, -F and –H and Additional File 8) between the two coral fractions. *spiSLC9A6* and *A7* (Fig. 6B and -C) are more highly expressed (p-value = 0.023 and 0.018, respectively) in the oral fraction, compared to the total colony, and *A8* (Fig. 6D) is higher expressed (p-value = 0.108) in the total colony, compared to the oral fraction. Finally, $spiH_vCN1.1$ (Fig. 6I) is more highly expressed (p-value = 0.107) in the total colony compared to the oral fraction, whereas $spiH_vCN1.2$ (Fig. 6L) is more highly expressed (p-value = 0.007) in the oral fraction compared to the total colony.

2.3 Effect of Ocean Acidification on Gene Expression of S. pistillata H^+ transporters

In order to study the effect of seawater acidification on H^+ transporters mRNA expression, real-time qPCR analysis on *spiSLC9A-B,* $spiV_0$ *V-ATPase subunit-a* and $spiH_vCNs$ genes was carried out on *S. pistillata* micro-colonies exposed to control and acidified seawater (pH 8.1 and 7.2, respectively) for two different time scales: one week and one year. Results show that there is no difference in expression between pH 8.1 and pH 7.2 after one-week exposure (Additional Files 9 and 11). After one-year exposure at lower pH, there is no difference in the expression of most H^+ transporters coding genes (Additional Files 10 and 11). Only *spiSLC9A1* is higher expressed (p-value = 0.029) at pH 7.2 compared to control condition (Additional File 11). Even if not significant, a general increase in gene expression at pH 7.2 can also be observed for the other *spiSLC9A-B* subfamily homologs.

3. Discussion

3.1.1 Phylogeny, Domain Topology and Motif Analysis of SLC9s from *S. pistillata*
We identified SLC9 homologs in all Anthozoa species (Fig. 1). Anthozoa SLC9 proteins cluster at least within one subfamily (A, B and C), previously described, suggesting a common ancestor at the time of Bilateria-Radiata separation.

spiSLC9s, characterized in *S. pistillata*, share similar characteristics to those of human SLC9s [25, 43], such as the highly homologous transmembrane domain and the variable cytosolic domain. In addition, several key residues, important for the functioning of hSLC9s, are also conserved in spiSLC9s. For the A subfamily (Additional File 4), these residues include: F161, which is important for Na^+ transport and acts as a pore-lining residue [44]; P167 and P168, which play a structural role in the folding of the transmembrane domain [45] and influence targeting and expression of SLC9A proteins [44]; and R440 and G455/G456, located in the so called “glycine rich region”, which contribute to proper functioning of the putative “pH_i sensor” domain [46]. For the B subfamily (Additional File 5) conserved features between human and *S. pistillata* homologs is especially apparent between glycine zipper (GZ) sequences. GZ sequences mediate close helix-helix folding within transmembrane structures and facilitate the formation of membrane pores. This feature might facilitate the access to the mitochondrial inner membrane, where these proteins are highly abundant [47]. Finally, the member of subfamily C (Additional File 6), contains two conserved domains, with the human homolog: the voltage-sensing domain (VSD) and the cyclic nucleotide-binding domain (CNBD). The VSD of spiSLC9C carries positively charged residues (K and R) in S4, which are strongly conserved also in the SLC9C of *Strongylocentrotus purpuratus*, *Ciona intestinalis*, *Lepisosteus oculatus* and *Drosophila melanogaster* [48]. Some of these residues are missing in *Homo sapiens*, suggesting that the voltage activation differs between these species and human. The CNBD also regulates the activity of spiSLC9C, probably through the binding of cyclic adenosine monophosphate (cAMP), produced by the soluble adenylyl cyclase enzyme (sAC), as reported in the sea urchin [48].

Overall, the conserved features of spiSLC9 support their identities as Na^+/H^+ exchangers. Common properties, to previously characterized SLC9s, sustain similar functionality and provide insights into their activation mechanism and regulation in *S. pistillata*.
3.1.2 Phylogeny, Domain Topology and Motif Analysis of V_0 V-ATPase subunit-a from S. pistillata
We identified V_0 V-ATPase subunit-a homologs in Anthozoa (Fig. 3). Contrary to most species, that possess more than one V_0 V-ATPase subunit-a homolog, Anthozoa possess only one. This suggests that the specialization of V_0 V-ATPase subunit-a homologs could be phylum-specific or even species-specific [49].

The V_0 V-ATPase subunit-a, characterized in *S. pistillata*, shares similar characteristics with those characterised in yeast and human, including the number of predicted TMs, that falls within the TMs range of its homologs (5–8 TMs) [50]. TMs are thought to form proton conducting hemichannels that allow H^+ to translocate across the membrane [51]. Previous studies, in yeast, allowed the identification of

functional residues in the V_0 V-ATPase subunit-a, through the use of random and site-direct mutagenesis. Among these, R735 is known to play an essential role in proton transport, as mutations of this residue result in complete inactivation of the ATP-dependent H^+ transport of the V-ATPase [26]. The conservation of this residue, in *S. pistillata*, suggests that R735 can fulfil its role in H^+ transport (Fig. 2B). Other residues (L739, H743, L746, E789, R799 and V803) involved in proton translocation and ATPase activity [50] are also conserved in *S. pistillata*.

Overall, the conserved features of spiV_0 V-ATPase subunit-a, with human and yeast homologs, support its identity as the subunit-a of the V_0 V-ATPase. Furthermore, the identification of homologs of all the V-ATPase subunits coding genes in the genome and transcriptome of *S. pistillata* (Additional File 7), suggests a conserved organisation between the *S. pistillata* V-ATPase and the human V-ATPase.

3.1.3 Phylogeny, Domain Topology and Motif Analysis of H_vCNs from *S. pistillata*

One H_vCN family member (H_vCN1.1) was identified in all species examined in this study, including the four anthozoan orders: Actinaria, Alcyonacea, Corallimorpharia and Scleractinia (Fig. 5). In addition, for the first time, we report a second member of the H_vCN family (H_vCN1.2), in some Cnidaria. Genomic and transcriptomic searches of H_vCN1.2, in public databases of Octocorallia and Hydrozoa (*Hydra magnipapillata*), did not produce any result (not shown). Selective expression of H_vCN1.2 only in Hexacorallia, suggests that it is specific to this cnidarian subclass and its presence as well in non-calcifying anthozoans (Corallimorphs and Actinaria) suggests that it is not linked to the appearance of aragonite biomineralization in Scleractinia [52]. The two voltage-gated proton channels, spiH_vCNs, characterized in *S. pistillata*, are highly divergent. This is further supported by the length of the phylogenetic branch (Fig. 5) that separates the two homologs: the amino acidic similarity is higher between spiH_vCN1.1 and hH_vCN1.1, than between spiH_vCN1.1 and spiH_vCN1.2.

spiH_vCNs possess molecular properties that are hallmarks of all H_vCNs, such as the four transmembrane segments, the basic (R) and acidic residues (D and E) associated with voltage-sensing, and the coiled-coil structure at the C-terminus [53]. The gating of proton channels is tightly regulated by pH and voltage, ensuring that they open only to extrude H^+ from the cell [37]. Phosphorylation of spiH_vCNs might activate these channels to open faster and at less positive voltages than those required without activation, as previously reported in human leukocytes [54–57].

SpiH_vCN1.1 and spiH_vCN1.2 share similar structure and organisation (Fig. 4). However, differences identified at the protein sequence level might reflect some unique features. First, many acidic residues, which are known to be associated with voltage sensing in hH_vCN1 [53, 59], are present in spiH_vCN1.1 and not in spiH_vCN1.2. This could result in a different sensitivity to voltage, with spiH_vCN1.2 being less sensitive compared to spiH_vCN1.1. Additionally, among these residues, D112 in S3, known to be essential for proton and charge selectivity [56], is missing and replaced by E112 in spiH_vCN1.2. However, a previous study demonstrated that the substitution of D112 with an acidic residue in the same position maintained proton specificity in hH_vCN1 [56], suggesting that both spiH_vCNs are proton specific. Another difference

concerns the Zn^{+2} binding residues of spiH_vCNs. It is known that, in human and mouse, proton currents are suppressed by extracellular Zn^{+2}, which binds to four Zn^{+2}-coordinating residues (E119, D123, H140 and H193) [60, 61]. By sequence comparison we observed that, at these positions, some residues are not conserved in spiH_vCN1.1 (H193G) and even less in spiH_vCN1.2 (E119L, D123E and H193K). Hence, we suggest that the replacement of the Zn^{+2}-coordinating residues with others, potentially affects spiH_vCNs Zn^{+2} sensitivity, as reported in vertebrates [62, 63]. Since spiH_vCN1.1 contains more Zn^{+2}-coordinating residues, we propose that it is more sensitive to Zn^{+2} than spiH_vCN1.2.

Overall, the conserved features of spiH_vCNs support their identities as voltage gated H^+-channels. Common properties of spiH_vCNs to hH_vCN sustain their voltage-sensitivity and proton specificity, with some differences concerning their Zn^{+2} sensitivity. In addition, distinctive properties between spiH_vCNs suggest different regulation, possibly linked to their localization/function. Future analyses, however, are required to validate these assumptions and provide insights into their physiological role.

3.2 Tissue-Specific Expression Patterns of H^+ transporters Genes in *S. pistillata*

Whole coral colonies are typically used in conventional techniques of gene expression analysis, limiting the possibility of further differentiating specific gene expression between oral and aboral tissues. These tissues contain different cell subtypes: some of them are more abundant (e.g. endosymbiotic dinoflagellates) or exclusively found (e.g. cells specialized for food digestion and reproduction, nematocysts) in the oral tissue, whereas others are exclusively found in the aboral tissue (e.g. calcifying cells) (Veron et al., 1993; Peter et al., 1997) [64]. As several physiological functions are associated to these cellular subtypes, analysing the differential gene expression of H^+ transporters in the two coral tissues helps identifying potential physiological processes in which they might take part.

In order to perform this task, we used a previously developed micro-dissection protocol [42, 65], to separate the oral fraction (including the oral disc and large part of the polyp body, with no or minimal contamination of the cells from the aboral tissue) from the total colony. We then compared the H^+ transporters expression in the oral fraction to the total expression of the total colony.

Our results demonstrate that some H^+ transporters are more expressed in the oral fraction, compared to the total colony (they will be called “oral-specific”); others are more expressed in the total colony, compared to the oral fraction (they will be called “aboral-specific”); and others are expressed at the same levels in both fractions (they will be called “ubiquitous”) (Fig. 6). Using the H^+ transporters tissue expression and the existing literature in other systems, as supporting information, we discuss the role that these transporters might play in corals.

The oral-specific H^+ transporters include: spiSLC9A6, spiSLC9A7 and spiH_vCN1.2 (Fig. 7). spiSLC9A6 and spiSLC9A7 are organellar homologs (Fig. 1) and, as reported for human [43, 66], they might play a role in

the vesicular neurotransmitters uptake, in the oral polyps, where an elaborated nerve ring system is present [67]. In addition, cells in the oral tissue are enriched with zooxanthellae [68], that produce and incorporate high levels of anion superoxide (O_2^-) and Zn^{+2}, which accumulate in the host cytoplasm [69–71]. In this regard, spiH_vCN1.2 might favour the exit of H^+ on the basolateral membrane of these cells, as reported in human osteoblasts [72], preventing membrane depolarization to extreme negative voltages associated to O_2^- electron transfer. To notice also that the lower sensitivity of spiH_vCN1.2 to Zn^{+2}, compared to spiH_vCN1.1 (see Discussion 3.1.3), could be correlated to the higher Zn^{+2} concentration levels in the oral (symbiotic) cells [63, 73–76].

The aboral specific H^+ transporters are spiH_vCN1.1 and spiSLC9A8 (Fig. 7). These transporters could play a role in the pH_i regulation of the calcifying cells. During the calcification reaction, H^+ are produced in the ECM which needs to be removed in order to promote an alkaline environment favourable for calcification [11, 77]. The Ca^{+2}-ATPase at the apical side of the calcifying cells has been suggested to be involved in this H^+ pumping out from the ECM [35]. On the basal side of the cell membrane, spiH_vCN1.1 might contribute to extrude excess of H^+ from the cytoplasm of calcifying cells, similar to the role it plays in coccolithophores [78]. Finally, the organellar spiSLC9A8 might regulate medial/trans-Golgi pH and intracellular trafficking like in human [79, 80], since in the calcifying cells this is particularly necessary for the regulation of the organic matrix synthesis and secretion [81].

The rest of the H^+ transporters (V_0 V-ATPase subunit-a, spiSLC9A1, -B1 and -B2) are ubiquitous (Fig. 7). Although our results suggest that the V_0 V-ATPase subunit-a is ubiquitously expressed throughout the coral tissues, the V_0 V-ATPase subunit-a isoforms, in human, have different tissue distribution with intracellular or apical/basolateral membrane localization [31, 50, 82–85]. However, as the primers used for the spiV_0 V-ATPase subunit-a detection did not discern among the different isoforms (X1, X2, X3 and X4, see Additional File 7), we cannot exclude a possible tissue specificity in the case of *S. pistillata*. For the other ubiquitous transporters, we suggest they play housekeeping roles. spiSLC9A1, for example, could play a role in homeostatic pH regulation, on the basolateral cell membrane, and spiSLC9B1-2 might participate to organismal ion homeostasis, on the mitochondrial inner membrane, as reported in vertebrates [19, 86–89]. Interestingly, spiSLC9A1 is the only transporter affected by seawater acidification, after one year of exposure (Additional File 10A). Its activation might be triggered by the pH_i sensor domain (see Discussion 3.1.1), which activates the transporter at low pH_i values, similar to human [19].

4. Conclusions

This study provides the first molecular characterization of the principal H^+ transporters involved in intracellular pH regulation and maintenance of cell physiological homeostasis. Most importantly, we report for the first time a novel member of the H_vCN gene family, H_vCN1.2, in the cnidarian subclass Hexacorallia. The involvement of H_vCN1.1 in H^+ transport and pH_i regulation raises the question of whether its newly identified homolog, H_vCN1.2, also participates in acid-base cellular homeostasis. This

can only be assessed by further functional studies (e.g. pharmacological experiments, electrophysiological measurements of H^+ currents, etc.) but the observed difference in H_VCNs expression pattern, in *S. pistillata* coral tissues, already suggests that the biological function of this gene family is more complex and varied than previously thought.

Moreover, we assessed the tissue-specificity of the H^+ transporters gene families in the coral *S. pistillata* and we observed that their expression was not restricted to only one specific tissue (oral or aboral) as reported for some members of the HCO_3^- gene family [20]. However, we observed higher or lower expression profiles in the oral or aboral tissues. These results both highlight the importance played by H^+ transporters in regulating homeostatic acid-base balance in the entire coral colony and indicate that the molecular tools for pH regulation of homeostatic (e.g. intracellular acid-base balance) and physiological processes (e.g. calcification, photosynthesis, food digestion, etc.) are common in the different coral tissues. Finally, we investigated the impact of OA on the H^+ transporters gene expression in *S. pistillata* and we identified one candidate gene (*spiSLC9A1*) involved in coral response to ocean acidification, showing differential expression under long term exposure to acidified seawater (one year). The influence of other environmental factors, e.g. temperature increase, remains to be tested as it will enrich information about coral phenotypic plasticity. This knowledge is especially relevant to our understanding of the ability of benthic animals to buffer the impacts of environmental changes, thereby providing more time for genetic adaptation to occur. In addition, responses to environmental changes are often species-specific (Venn et al., 2019), with physiological differences that can potentially reflect a different profile of H^+ transporters gene expression, which could be investigated also in other coral species. Such comparative studies might aid in the development of molecular markers linked to pH_i tolerant traits in the coral reef population.

Methods

Biological materials Experiments were conducted on the symbiotic scleractinian coral *Stylophora pistillata* grown in the long-term culture facilities at the Centre Scientifique de Monaco, in aquaria supplied with seawater from the Mediterranean Sea (exchange rate 2% h − 1), under controlled conditions: semi-open circuit, temperature of 25 °C, salinity of 38, light of 200 µmol photons m^{-2} s^{-1} on a 12h:12 h light:dark cycle. Samples were prepared from one mother colony as nubbins suspended on monofilament threads. After three weeks of cicatrisation, a first set of samples (n = 3) was used for the “Oral fraction micro-dissection” experiment and another (n = 20) for “Exposure to seawater acidification” experiment.

Exposure to seawater acidification The seawater acidification setup was performed as described previously (Liew et al. 2017; Tambutté et al. 2015; Venn et al. 2019). Briefly, carbonate chemistry was manipulated by bubbling with CO_2 to reduce pH to the target value 7.2, compared to the control treatment (pH 8.1). 20 coral nubbins were randomly distributed between four experimental tanks (n = 5 for each experimental tank): two tanks (pH 8.1 and 7.2) were reserved for one-week exposure and two for one-year

exposure. Experiments were repeated three times to ensure reliability. Each time similar results were obtained (not shown).

Data mining Amino acidic sequences of human H^+ transporters were retrieved from NCBI (http://www.ncbi.nlm.nih.gov/protein) and used as a bait to mine (BLAST) the transcriptome, genome and EST databases of the following phyla: Cnidaria (*Stylophora pistillata*, *Acropora digitifera*, *Nematostella vectensis*, *Aiptasia pallida*, *Amplexidiscus fenestrafer*, *Discosoma sp.*, *Corallium rubrum* and *Dendronephythya gigantea*), Mollusca (*Crassostrea gigas*), Echinodermata (*Strongylocentrotus purpuratus*), Chordata (*Ciona intestinalis*), Porifera (*Sycon ciliatum*) and Placozoa (*Trichoplax adhaerens*), using the listed web servers: NCBI (http://www.ncbi.nlm.nih.gov/), EnsemblMetazoa (https://metazoa.ensembl.org/), ReefGenomics (http://reefgenomics.org) and Cnidarian Database (http://data.centrescientifique.mc/).

Sequence analysis Putative transmembrane helices in proteins were predicted on the Center for Biological Sequence analysis prediction server (http://www.cbs.dtu.dk/services/) using TMHMM algorithm. On the same platform, phosphorylation and N-glycosylation prediction analysis were performed as well using NetPhos and NetNGlyc.

Phylogenetic analyses The alignment of H^+ transporters amino acid sequences was performed using Clustal Omega on the EMBL-EBI server (https://www.ebi.ac.uk/). Based upon the produced amino acid alignments, maximum likelihood estimates of the topology and the branch length were obtained using PhyML v3.1 [92]. The model of substitution used in this step was LG + G, which was previously selected over others by alignment analysis with ProtTest3.4.2 [93]. Phylogenetic trees were then edited using FigTreev1.4.4 (Rambaut et al., 2014).

Oral fraction micro-dissection Coral micro-dissection was performed as indicated previously [20, 42]. Briefly, coral nubbins ($n = 3$) were set to rest in a glass petri dish filled with seawater and tricaine mesylate. Once polyps were extended, oral fractions (including the oral disc and large part of the polyp body) were cut, using microdissection scissors, from the coral colony (total colony), under a binocular microscope. Both fractions (oral fraction and total colony) were then used for RNA extractions.

Real-time PCR (qPCR) Total RNA extraction and cDNA synthesis were performed as described previously [94]. Briefly, RNA was isolated from triplicates undergone micro-dissection or from quintuplicates collected for each pH treatments using RNeasy kit (Qiagen), according to manufacturer's instructions. Reverse transcription was then performed using Invitrogen's SuperScript IV Reverse Transcriptase on 2 µg of RNA. Thermo cycler conditions were set as follows: 50 minutes at 50 °C, 7 minutes at 25 °C, 50 minutes at 50 °C and 5 minutes at 85 °C. qPCR runs were performed in 96-wells plates on the QuantStudio 3 (Applied Biosystems) machine, using PowerUpTM SYBRTM Green Master Mix for PCR amplification. Primer sequences used are given in Additional File 12. Relative expression was calculated using Biogazelle qBase + 2.6TM [95]. Gene expression was normalized (relative mRNA quantification-R_q) to ubiquitin-60S ribosomal protein (L40) [96] and an acidic ribosomal phosphoprotein P0 (36B4) [97].

Statistical analysis Statistical analysis was performed using R v3.5.2 software. For the “Oral fraction micro-dissection” experiment a fixed number of samples ($n = 3$) was used due to technical limitations. Whereas for the “Exposure to seawater acidification” experiment, a sample size estimation was performed and $n = 5$ samples were used. For both experiments, the normal distribution of the data was evaluated using the Shapiro-Wilk’s test. Samples with standard deviation ≥ 5 were excluded from the analysis. This was the case for *spiSLC9C*, whose qPCR results showed great variability probably due to its extremely low expression values. One-way ANOVA was used to identify differentially expressed genes between *S. pistillata* fractions (oral fraction and total colony) and pH treatments (8.1 and 7.2). We considered 0.11 ≤ p-values ≤ 0.10 near the marginal significance (Ÿ); p-values ≤ 0.1 significant (**); and p-values ≤ 0.05 highly significant (*).

Declarations

Ethics approval and consent to participate

Not applicable.

Consent for publication

Not applicable.

Availability of data and materials

All data needed to evaluate the conclusions in the paper are present in the manuscript and/or the Additional Files. Additional data related to this manuscript may be requested from the authors. Genomic and transcriptomic data were obtained from the public available database of the National Center for Biotechnology Information or from the private database of the Centre Scientifique de Monaco.

Competing interests

The authors declare that they have no competing interests.

Funding

Funding of this study was supported by the Government of the Principality of Monaco

Authors’ contributions

ST and DZ designed and conceived the study. LC conducted the study. LC, PG, VPB and DZ analysed the data. LC, ST and DZ wrote the manuscript. All authors read and approved the manuscript.

Acknowledgments

We would like to thank Dominique Desgré for coral maintenance and Alexander Venn for kindly revisioning the text of the manuscript. This study was conducted as part of the Centre Scientifique de

Monaco research program, supported by the Government of the Principality of Monaco.

References

1. Mumby PJ, Steneck RS. Coral reef management and conservation in light of rapidly evolving ecological paradigms. Trends Ecol Evol. 2008;23:555–63.
2. Davies PS. Effect of daylight variations on the energy budgets of shallow-water corals. Mar Biol. 1991;108:137–44.
3. Tambutté S, Tambutté E, Zoccola D, Allemand D. Organic Matrix and Biomineralization of Scleractinian Corals. Handb Biominer Biol Asp Struct Form. 2008;1:243–59.
4. Davy SK, Allemand D, Weis VM. Cell Biology of Cnidarian-Dinoflagellate Symbiosis. Microbiol Mol Biol Rev. 2012;76:229–61.
5. Kleypas JA, Buddemeier RW, Archer D, Gattuso J, Langdon C, Opdyke BN, et al. Geochemical Consequences of Increased Atmospheric Carbon Dioxide on Coral Reefs Published by : American Association for the Advancement of Science Stable URL : http://www.jstor.org/stable/2899149 Linked references are available on JSTOR for this article : 1999;284:118–20.
6. Chan NCS, Connolly SR. Sensitivity of coral calcification to ocean acidification: A meta-analysis. Glob Chang Biol. 2013;19:282–90.
7. Schoepf V, Grottoli AG, Warner ME, Cai WJ, Melman TF, Hoadley KD, et al. Coral Energy Reserves and Calcification in a High-CO2 World at Two Temperatures. PLoS One. 2013;8.
8. Comeau S, Cornwall CE, McCulloch MT. Decoupling between the response of coral calcifying fluid pH and calcification to ocean acidification. Sci Rep. 2017;7:1–10. doi:10.1038/s41598-017-08003-z.
9. Venn AA, Tambutté E, Caminiti-Segonds N, Techer N, Allemand D, Tambutté S. Effects of light and darkness on pH regulation in three coral species exposed to seawater acidification. Sci Rep. 2019;9:1–12.
10. Tresguerres M, Hamilton TJ. Acid-base physiology, neurobiology and behaviour in relation to CO2-induced ocean acidification. J Exp Biol. 2017;220:2136–48.
11. Allemand D, Ferrier-Pagès C, Furla P, Houlbrèque F, Puverel S, Reynaud S, et al. Biomineralisation in reef-building corals: From molecular mechanisms to environmental control. Comptes Rendus - Palevol. 2004;3:453–67.
12. Webb DJ, Nuccitelli R. Fertilization potential and electrical properties of the Xenopus laevis egg. Dev Biol. 1985;107:395–406.
13. Venn AA, Tambutté E, Lotto S, Zoccola D, Allemand D, Tambutté S. Imaging intracellular pH in a reef coral and symbiotic anemone. Proc Natl Acad Sci U S A. 2009;106:16574–9.
14. Laurent J, Tambutté S, Tambutté É, Allemand D, Venn A. The influence of photosynthesis on host intracellular ph in scleractinian corals. J Exp Biol. 2013;216:1398–404.
15. Al-Horani FA, Al-Moghrabi SM, De Beer D. The mechanism of calcification and its relation to photosynthesis and respiration in the scleractinian coral Galaxea fascicularis. Mar Biol.

2003;142:419–26.

16. Agostini S, Suzuki Y, Higuchi T, Casareto BE, Yoshinaga K, Nakano Y, et al. Biological and chemical characteristics of the coral gastric cavity. Coral Reefs. 2012;31:147–56.
17. Cai WJ, Ma Y, Hopkinson BM, Grottoli AG, Warner ME, Ding Q, et al. Microelectrode characterization of coral daytime interior pH and carbonate chemistry. Nat Commun. 2016;7:1–8.
18. Bove CB, Whitehead RF, Szmant AM. Responses of coral gastrovascular cavity pH during light and dark incubations to reduced seawater pH suggest species-specific responses to the effects of ocean acidification on calcification. Coral Reefs. 2020. doi:10.1007/s00338-020-01995-7.
19. Casey JR, Grinstein S, Orlowski J. Sensors and regulators of intracellular pH. Nat Rev Mol Cell Biol. 2010;11:50–61. doi:10.1038/nrm2820.
20. Zoccola D, Ganot P, Bertucci A, Caminiti-Segonds N, Techer N, Voolstra CR, et al. Bicarbonate transporters in corals point towards a key step in the evolution of cnidarian calcification. Sci Rep. 2015;5. doi:10.1038/srep09983.
21. Barott KL, Barron ME, Tresguerres M. Identification of a molecular pH sensor in coral. Proc R Soc B Biol Sci. 2017;284.
22. Tresguerres M, Barott KL, Barron ME, Deheyn DD, Kline DI, Linsmayer LB. Acid-Base Balance and Nitrogen Excretion in Invertebrates. Acid-Base Balanc Nitrogen Excretion Invertebr. 2017;:193–218.
23. Nishigaki T, José O, González-Cota AL, Romero F, Treviño CL, Darszon A. Intracellular pH in sperm physiology. Biochem Biophys Res Commun. 2014;450:1149–58. doi:10.1016/j.bbrc.2014.05.100.
24. Orlowski J, Grinstein S. Diversity of the mammalian sodium/proton exchanger SLC9 gene family. Pflugers Arch Eur J Physiol. 2004;447:549–65.
25. Donowitz M, Ming Tse C, Fuster D. SLC9/NHE gene family, a plasma membrane and organellar family of Na +/H+ exchangers. Mol Aspects Med. 2013;34:236–51.
26. Kawasaki-Nishi S, Nishi T, Forgac M. Arg-735 of the 100-kDa subunit a of the yeast V-ATPase is essential for proton translocation. Proc Natl Acad Sci U S A. 2001;98:12397–402.
27. Salvador JM, Inesi G, Rigaud JL, Mata AM. Ca2+ transport by reconstituted synaptosomal ATPase is associated with H+ countertransport and net charge displacement. J Biol Chem. 1998;273:18230–4.
28. Brini M, Carafoli E, Rosenberg SS, Spitzer NC, Fearnley CJ, Roderick HL, et al. The Plasma Membrane Ca 2 þ ATPase and the Cooperate in the Regulation of Cell Calcium. 2012.
29. Perry SF, Beyers ML, Johnson DA. Cloning and molecular characterisation of the trout (Oncorhynchus mykiss) vacuolar H+-ATPase B subunit. J Exp Biol. 2000;203:459–70.
30. Torigoe T, Izumi H, Ise T, Murakami T, Uramoto H, Ishiguchi H, et al. Vacuolar H+-ATPase: Functional mechanisms and potential as a target for cancer chemotherapy. Anticancer Drugs. 2002;13:237–43.
31. Miranda KC, Karet FE, Brown D. An extended nomenclature for mammalian V-ATPase subunit genes and splice variants. PLoS One. 2010;5:1–5.
32. Tresguerres M, Clifford AM, Harter TS, Roa JN, Thies AB, Yee DP, et al. Evolutionary links between intra- and extracellular acid–base regulation in fish and other aquatic animals. J Exp Zool Part A

Ecol Integr Physiol. 2020;333:449–65.
33. DeCoursey TE. Voltage-gated proton channels. Cell Mol Life Sci. 2008;65:2554–73.
34. Lishko P V., Botchkina IL, Fedorenko A, Kirichok Y. Acid Extrusion from Human Spermatozoa Is Mediated by Flagellar Voltage-Gated Proton Channel. Cell. 2010;140:327–37.
35. Zoccola D, Tambutté E, Kulhanek E, Puverel S, Scimeca JC, Allemand D, et al. Molecular cloning and localization of a PMCA P-type calcium ATPase from the coral Stylophora pistillata. Biochim Biophys Acta - Biomembr. 2004;1663:117–26.
36. Barott KL, Venn AA, Perez SO, Tambutteeé S, Tresguerres M, Somero GN. Coral host cells acidify symbiotic algal microenvironment to promote photosynthesis. Proc Natl Acad Sci U S A. 2015;112:607–12.
37. Decoursey TE. Voltage-gated proton channels and other proton transfer pathways. Physiol Rev. 2003;83:475–579.
38. Forgac M. Vacuolar ATPases: Rotary proton pumps in physiology and pathophysiology. Nat Rev Mol Cell Biol. 2007;8:917–29.
39. Wang Y, Li SJ, Wu X, Che Y, Li Q. Clinicopathological and biological significance of human voltage-gated proton channel Hv1 protein overexpression in breast cancer. J Biol Chem. 2012;287:13877–88.
40. Voolstra CR, Li Y, Liew YJ, Baumgarten S, Zoccola D, Flot JF, et al. Comparative analysis of the genomes of Stylophora pistillata and Acropora digitifera provides evidence for extensive differences between species of corals. Sci Rep. 2017;7.
41. Karako-Lampert S, Zoccola D, Salmon-Divon M, Katzenellenbogen M, Tambutté S, Bertucci A, et al. Transcriptome analysis of the scleractinian coral stylophora pistillata. PLoS One. 2014;9.
42. Ganot P, Zoccola D, Tambutté E, Voolstra CR, Aranda M, Allemand D, et al. Structural Molecular Components of Septate Junctions in Cnidarians Point to the Origin of Epithelial Junctions in Eukaryotes. Mol Biol Evol. 2015;32:44–62.
43. Fuster DG, Alexander RT. Traditional and emerging roles for the SLC9 Na+/H+ exchangers. Pflugers Arch Eur J Physiol. 2014;466:61–76.
44. Slepkov ER, Chow S, Lemieux MJ, Fliegel L. Proline residues in transmembrane segment IV are critical for activity, expression and targeting of the Na+/H+ exchanger isoform 1. Biochem J. 2004;379:31–8.
45. Counillon L, Franchi A, Pouyssegur J. A point mutation of the Na+/H+ exchanger gene (NHE1) and amplification of the mutated allele confer amiloride resistance upon chronic acidosis. Proc Natl Acad Sci U S A. 1993;90:4508–12.
46. Wakabayashi S, Hisamitsu T, Pang T, Shigekawa M. Mutations of Arg440 and Gly455/Gly456 oppositely change pH sensing of Na+/H+ exchanger 1. J Biol Chem. 2003;278:11828–35.
47. Holmes RS, Spradling Reeves KD. Evolution of Vertebrate Solute Carrier Family 9B Genes and Proteins (SLC9B): Evidence for a Marsupial Origin for Testis Specific SLC9B1 from an Ancestral Vertebrate SLC9B2 Gene. J Phylogenetics Evol Biol. 2016;4:1–8.

48. Windler F, Bönigk W, Körschen HG, Grahn E, Strünker T, Seifert R, et al. The solute carrier SLC9C1 is a Na+/H+-exchanger gated by an S4-type voltage-sensor and cyclic-nucleotide binding. Nat Commun. 2018;9:1–13. doi:10.1038/s41467-018-05253-x.
49. Smith AN, Finberg KE, Wagner CA, Lifton RP, Devonald MAJ, Su Y, et al. Molecular Cloning and Characterization of Atp6n1b. A novel fourth murine vacuolar H+-ATPase a-subunit gene. J Biol Chem. 2001;276:42382–8.
50. Leng XH, Manolson MF, Forgac M. Function of the COOH-terminal domain of Vph1p in activity and assembly of the yeast V-ATPase. J Biol Chem. 1998;273:6717–23.
51. Cotter K, Stransky L, McGuire C, Forgac M. Recent Insights into the Structure, Regulation, and Function of the V-ATPases. Trends Biochem Sci. 2015;40:611–22. doi:10.1016/j.tibs.2015.08.005.
52. Jr GDS. Cloud Thinking - Simplifying Big Data Processing. Target Conf 2013, Probing Big Data answers. 2013;60:195–225.
53. DeCoursey TE. Voltage and pH sensing by the voltage-gated proton channel, HV1. J R Soc Interface. 2018;15.
54. Bánfi B, Schrenzel J, Nüsse O, Lew DP, Ligeti E, Krause KH, et al. A novel H+ conductance in eosinophils: Unique characteristics and absence in chronic granulomatous disease. J Exp Med. 1999;190:183–94.
55. DeCoursey TE, Cherny V V., Zhou W, Thomas LL. Simultaneous activation of NADPH oxidase-related proton and electron currents in human neutrophils. Proc Natl Acad Sci U S A. 2000;97:6885–9.
56. Musset B, Smith SME, Rajan S, Morgan D, Cherny V V., Decoursey TE. Aspartate 112 is the selectivity filter of the human voltage-gated proton channel. Nature. 2011;480:273–7. doi:10.1038/nature10557.
57. Capasso M, DeCoursey TE, Dyer MJS. PH regulation and beyond: Unanticipated functions for the voltage-gated proton channel, HVCN1. Trends Cell Biol. 2011;21:20–8. doi:10.1016/j.tcb.2010.09.006.
58. Musset B, Capasso M, Cherny V V., Morgan D, Bhamrah M, Dyer MJS, et al. Identification of Thr29 as a critical phosphorylation site that activates the human proton channel Hvcn1 in leukocytes. J Biol Chem. 2010;285:5117–21.
59. Stühmer W, Conti F, Suzuki H, Wang X, Noda M, Yahagi N, et al. Structural parts involved in activation and inactivation of the sodium channel. Nature. 1989;339:597–603.
60. Ramsey IS, Moran MM, Chong JA, Clapham DE. A voltage-gated proton-selective channel lacking the pore domain. Nature. 2006;440:1213–6.
61. Takeshita K, Sakata S, Yamashita E, Fujiwara Y, Kawanabe A, Kurokawa T, et al. X-ray crystal structure of voltage-gated proton channel. Nat Struct Mol Biol. 2014;21:352–7. doi:10.1038/nsmb.2783.
62. Sasaki M, Takagi M, Okamura Y. A voltage sensor-domain protein is a voltage-gated proton channel. Science (80-). 2006;312:589–92.

63. Ratanayotha A, Kawai T, Higashijima SI, Okamura Y. Molecular and functional characterization of the voltage-gated proton channel in zebrafish neutrophils. Physiol Rep. 2017;5.
64. Rosental B, Kozhekbaeva Z, Fernhoff N, Tsai JM, Traylor-Knowles N. Coral cell separation and isolation by fluorescence-activated cell sorting (FACS). BMC Cell Biol. 2017;18:1–12.
65. Zoccola D, Ganot P, Bertucci A, Caminiti-Segonds N, Techer N, Voolstra CR, et al. Bicarbonate transporters in corals point towards a key step in the evolution of cnidarian calcification. Sci Rep. 2015;5.
66. Zhao H, Carney KE, Falgoust L, Pan JW, Sun D, Zhang Z. Emerging roles of Na+/H+ exchangers in epilepsy and developmental brain disorders. Prog Neurobiol. 2016;138–140:19–35. doi:10.1016/j.pneurobio.2016.02.002.
67. Watanabe H, Fujisawa T, Holstein TW. Cnidarians and the evolutionary origin of the nervous system. Dev Growth Differ. 2009;51:167–83.
68. Furla P, Allemand D, Shick JM, Ferrier-Pagès C, Richier S, Plantivaux A, et al. The symbiotic anthozoan: A physiological chimera between alga and animal. Integr Comp Biol. 2005;45:595–604.
69. Saragosti E, Tchernov D, Katsir A, Shaked Y. Extracellular production and degradation of superoxide in the coral stylophora pistillata and cultured symbiodinium. PLoS One. 2010;5:1–10.
70. Zhang T, Diaz JM, Brighi C, Parsons RJ, McNally S, Apprill A, et al. Dark production of extracellular superoxide by the coral Porites astreoides and representative symbionts. Front Mar Sci. 2016;3 NOV:1–16.
71. Raz-Bahat M, Douek J, Moiseeva E, Peters EC, Rinkevich B. The digestive system of the stony coral Stylophora pistillata. Cell Tissue Res. 2017;368:311–23.
72. Mészáros B, Papp F, Mocsár G, Kókai E, Kovács K, Tajti G, et al. The voltage-gated proton channel hHv1 is functionally expressed in human chorion-derived mesenchymal stem cells. Sci Rep. 2020;10:1–16.
73. Harland AD, Brown BE. Metal tolerance in the scleractinian coral Porites lutea. Mar Pollut Bull. 1989;20:353–7.
74. Reichelt-Brushett AJ, McOrist G. Trace metals in the living and nonliving components of scleractinian corals. Mar Pollut Bull. 2003;46:1573–82.
75. Ferrier-Pagès C, Houlbrèque F, Wyse E, Richard C, Allemand D, Boisson F. Bioaccumulation of zinc in the scleractinian coral Stylophora pistillata. Coral Reefs. 2005;24:636–45.
76. Murphy R, DeCoursey TE. Charge compensation during the phagocyte respiratory burst. Biochim Biophys Acta - Bioenerg. 2006;1757:996–1011.
77. Venn A, Tambutté E, Holcomb M, Allemand D, Tambutté S. Live tissue imaging shows reef corals elevate pH under their calcifying tissue relative to seawater. PLoS One. 2011;6.
78. Taylor AR, Chrachri A, Wheeler G, Goddard H, Brownlee C. A voltage-gated H+ channel underlying pH homeostasis in calcifying Coccolithophores. PLoS Biol. 2011;9:1–14.

79. Lawrence SP, Holman GD, Koumanov F. Translocation of the Na+/H+ exchanger 1 (NHE1) in cardiomyocyte responses to insulin and energy-status signalling. Biochem J. 2010;432:515–23.
80. Xia CH, Liu H, Cheung D, Tang F, Chang B, Li M, et al. NHE8 Is Essential for RPE Cell Polarity and Photoreceptor Survival. Sci Rep. 2015;5:1–8.
81. Puverel S, Tambutté E, Zoccola D, Domart-Coulon I, Bouchot A, Lotto S, et al. Antibodies against the organic matrix in scleractinians: A new tool to study coral biomineralization. Coral Reefs. 2005;24:149–56.
82. Nishi T, Forgac M. The vacuolar (H+)-ATPases - Nature's most versatile proton pumps. Nat Rev Mol Cell Biol. 2002;3:94–103.
83. Smith AN, Lovering RC, Futai M, Takeda J, Brown D, Karet FE. Revised nomenclature for mammalian vacuolar-type H+-ATPase subunit genes. Mol Cell. 2003;12:801–3.
84. Toei M, Saum R, Forgac M. Regulation and isoform function of the V-ATPases. Biochemistry. 2010;49:4715–23.
85. Toyomura T, Oka T, Yamaguchi C, Wada Y, Futai M. Three subunit a isoforms of mouse vacuolar H+-ATPase. Preferential expression of the α3 isoform during osteoclast differentiation. J Biol Chem. 2000;275:8760–5.
86. Xiang M, Feng M, Muend S, Rao R. A human Na+/H+ antiporter sharing evolutionary origins with bacterial NhaA may be a candidate gene for essential hypertension. Proc Natl Acad Sci U S A. 2007;104:18677–81.
87. Fuster DG, Zhang J, Shi M, Alexandru Bobulescu I, Andersson S, Moe OW. Characterization of the sodium/hydrogen exchanger NHA2. J Am Soc Nephrol. 2008;19:1547–56.
88. S Holmes R. Evolution of Mammalian KELL Blood Group Glycoproteins and Genes (KEL): Evidence for a Marsupial Origin from an Ancestral M13 Type II Endopeptidase Gene. J Phylogenetics Evol Biol. 2013;01:1–9.
89. Pedersen SF, Counillon L. The SLC9A-C mammalian Na+/H+ exchanger family: Molecules, mechanisms, and physiology. Physiol Rev. 2019;99:2015–113.
90. Liew YJ, Zoccola D, Li Y, Tambutté E, Venn A, Michell C, et al. Epigenome-associated phenotypic acclimatization to ocean acidification in a reef-building coral. bioRxiv. 2017; December 2016:188227.
91. Tambutté E, Venn AA, Holcomb M, Segonds N, Techer N, Zoccola D, et al. Morphological plasticity of the coral skeleton under CO2-driven seawater acidification. Nat Commun. 2015;6.
92. Guindon S. Bayesian estimation of divergence times from large sequence alignments. Mol Biol Evol. 2010;27:1768–81.
93. Darriba D, Taboada GL, Doallo R, Posada D. ProtTest 3: Fasfile:///Users/Laura/Downloads/gb-2007-8-2-r19.pdft selection of best-fit models of protein file:///Users/Laura/Downloads/gb-2007-8-2-r19.pdfevolution. Bioinformatics. 2011;27:1164–5.
94. Bernardet C, Tambutté E, Techer N, Tambutté S, Venn AA. Ion transporter gene expression is linked to the thermal sensitivity of calcification in the reef coral Stylophora pistillata. Sci Rep. 2019;9:1–13.

95. Hellemans J, Mortier G, De Paepe A, Speleman F, Vandesompele J. qBase relative quantification framework and software for management and automated analysis of real-time quantitative PCR data. Genome Biol. 2008;8.
96. Zoccola D, Innocenti A, Bertucci A, Tambutté E, Supuran CT, Tambutté S. Coral carbonic anhydrases: Regulation by ocean acidification. Mar Drugs. 2016;14.
97. Moya A, Tambutté S, Bertucci A, Tambutté E, Lotto S, Vullo D, et al. Carbonic anhydrase in the scleractinian coral Stylophora pistillata: Characterization, localization, and role in biomineralization. J Biol Chem. 2008;283:25475–84.

Figures

Figure 1

A maximum likelihood phylogenetic (Phyml, LG+I+G) tree of human and cnidarian SLC9s (protein sequences were previously aligned by Clustal Omega). Phylogenetic analysis of S. pistillata SLC9 sequences with functionally characterized SLC9s in H. sapiens grouped cnidarian SLC9s within three different subfamilies: subfamily A, including plasma membrane and organelle homologs, represented in

blue and red respectively; subfamily B represented in orange and subfamily C represented in yellow. Cnidarian species include: Stylophora pistillata (Spi), Acropora digitifera (Adi), Nematostella vectensis (Nve), Aiptasia pallida (Apa), Corallium rubrum (Cru), Dendronephythya gigantea (Dgi), Amplexidiscus fenestrafer (Afe), Discosoma sp. (Dsp). Chordata species include Homo sapiens (Hsa).

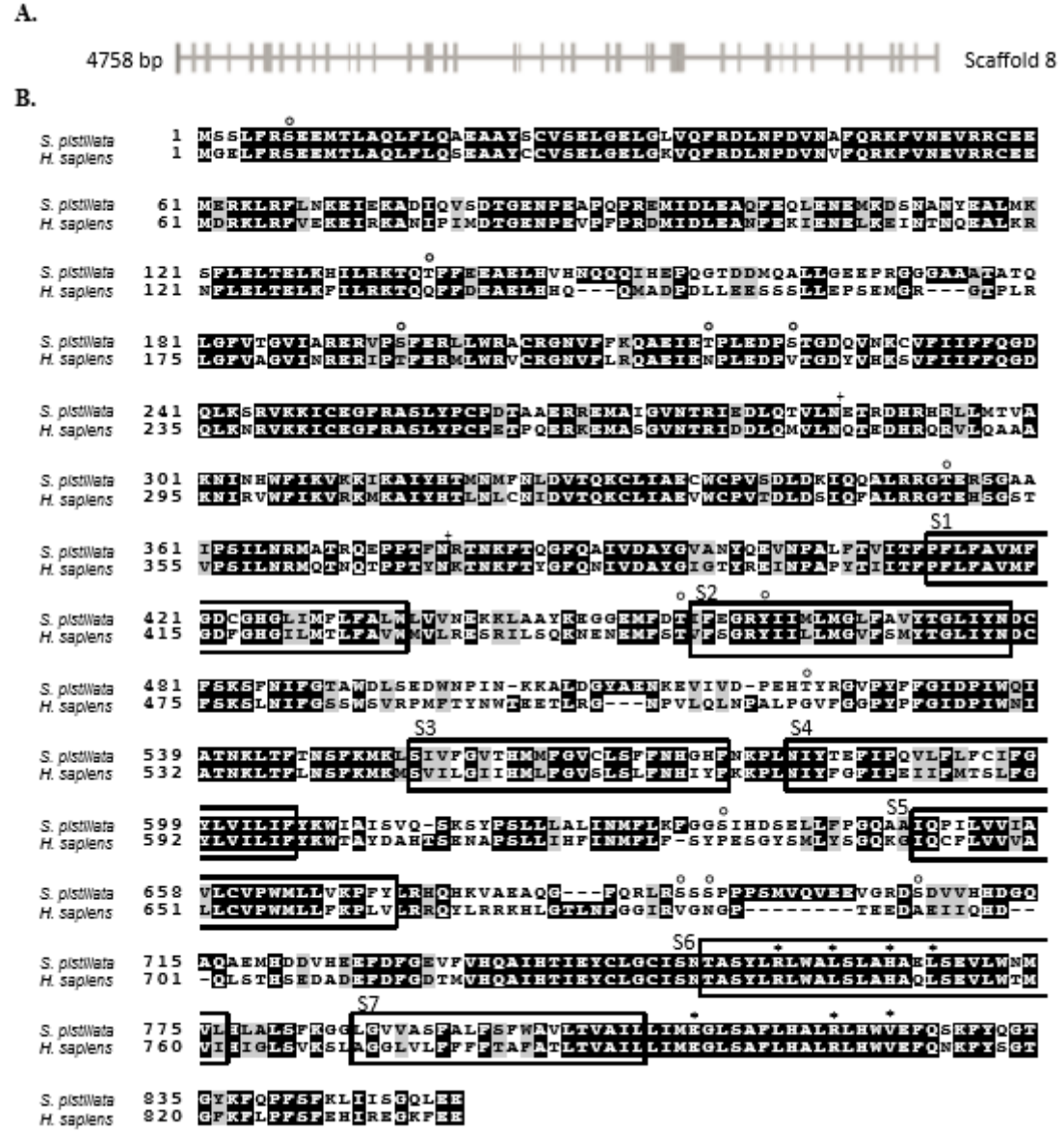

Figure 2

A. Exon/intron organization of V0 V-ATPase subunit a in the genome of S. pistillata. Exons are represented as boxes whereas introns are depicted as lines. B. Sequence comparison of S. pistillata and H. sapiens V0 V-ATPase subunit a. Identical and similar amino acids (aa) are shaded in black and grey, respectively. Boxes represent predicted transmembrane segments in H. sapiens V0 V-ATPase subunit a. Circles and crosses represent phosphorylation and N-glycosylation sites, respectively, in spiHvCN1.1 and spiHvCN1.2. Asterisk indicates conserved R relevant for H+ transport.

Figure 3

Maximum Likelihood (Phyml, LG+I+G) phylogenetic tree of the V0 V-ATPase subunit-a (protein sequences were previously aligned by Clustal Omega). Cnidarian species include: Stylophora pistillata (Spi), Acropora digitifera (Adi), Nematostella vectensis (Nve), Aiptasia pallida (Apa), Corallium rubrum (Cru), Dendronephythya gigantea (Dgi), Amplexidiscus fenestrafer (Afe), Discosoma sp. (Dsp). Mollusca species include: Crassostrea gigas (Cgi). Echinodermata species include: Strongylocentrotus purpuratus (Spu) and Acanthaster planci (Apl). Chordata species include Homo sapiens (Hsa) and Ciona intestinalis (Cin). Placozoa species include Trichoplax adhaerens (Tad). Porifera calcarea species include Sycon ciliatum (Sci). Porifera Homoscleromorpha species include Oscarella carmela (Oca).

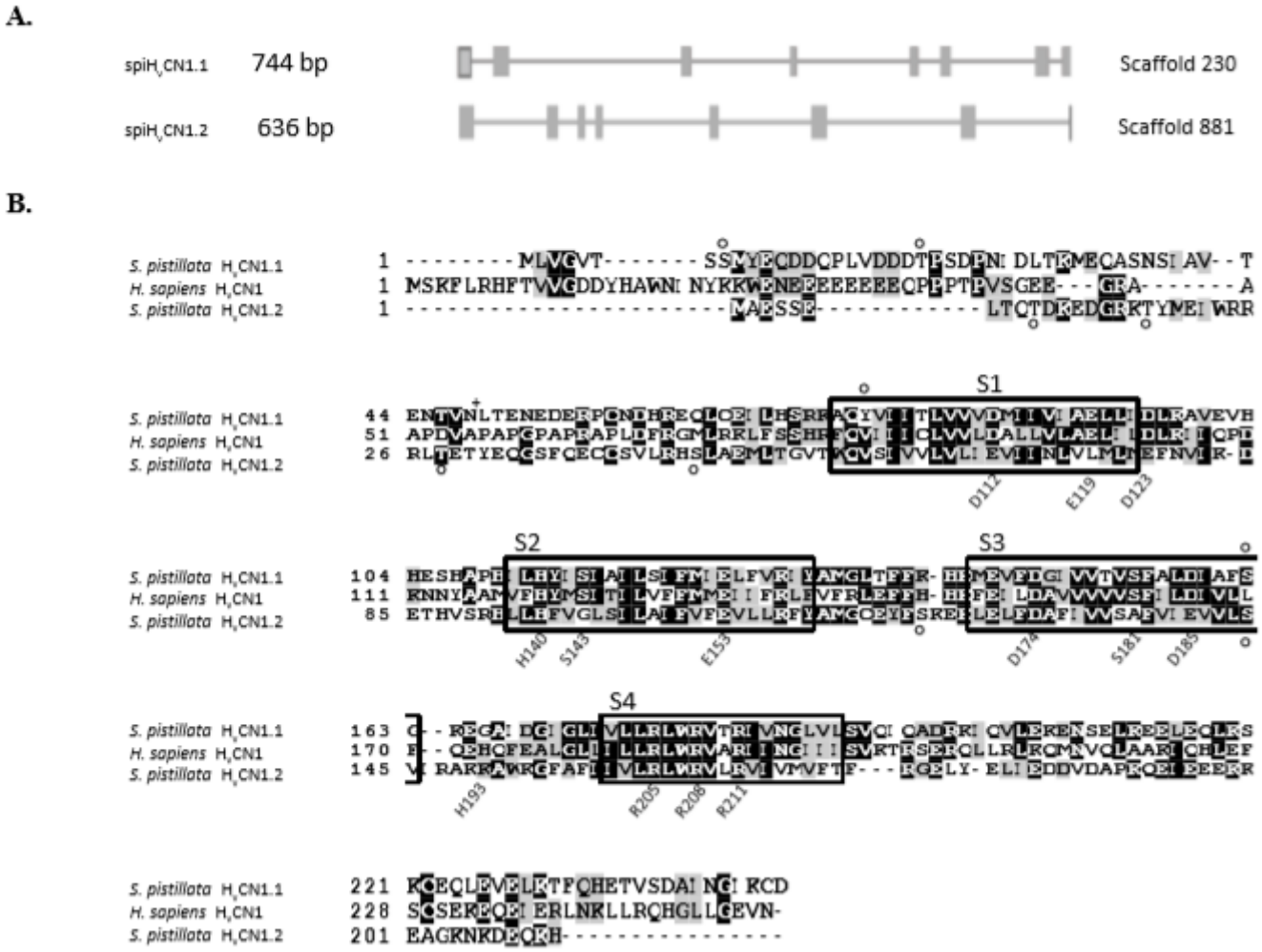

Figure 4

A. Exon/intron organization of spiHvCNs in the genome of S. pistillata. Exons are represented as boxes whereas introns are depicted as lines. B. Sequence comparison of S. pistillata and H. sapiens HvCN proteins. Identical and similar amino acids (aa) are shaded in black and grey, respectively, whereas aa that are missing from the other sequence are denoted by dashes. Boxes represent predicted transmembrane segments in human HvCN1 (S1-S4). Circles and crosses represent phosphorylation and N-glycosylation sites, respectively, in spiHvCN1.1 and spiHvCN1.2.

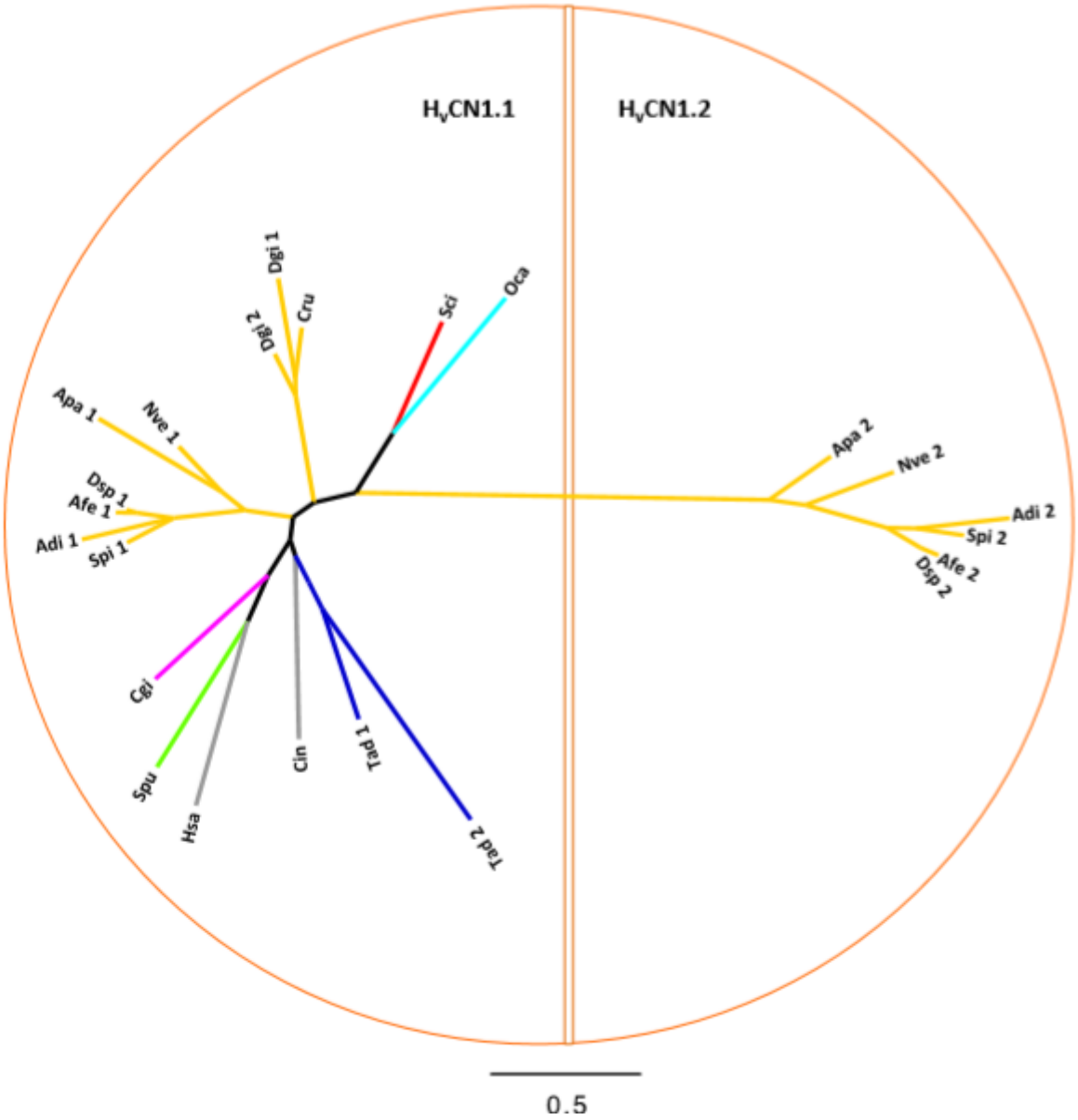

Figure 5

Maximum Likelihood (Phyml, LG+I+G) phylogenetic tree of voltage-gated proton channels (protein sequences were previously aligned by Clustal Omega). HvCN1.1 and HvCN1.2 are separated in two semicircles. Cnidarian species include: Stylophora pistillata (Spi), Acropora digitifera (Adi), Nematostella vectensis (Nve), Aiptasia pallida (Apa), Corallium rubrum (Cru), Dendronephythya gigantea (Dgi), Amplexidiscus fenestrafer (Afe), Discosoma sp. (Dsp). Mollusca species include: Crassostrea gigas (Cgi). Echinodermata species include: Strongylocentrotus purpuratus (Spu) and Acanthaster planci (Apl). Chordata species include Homo sapiens (Hsa) and Ciona intestinalis (Cin). Placozoa species include Trichoplax adhaerens (Tad). Porifera calcarea species include Sycon ciliatum (Sci). Porifera Homoscleromorpha species include Oscarella carmela (Oca).

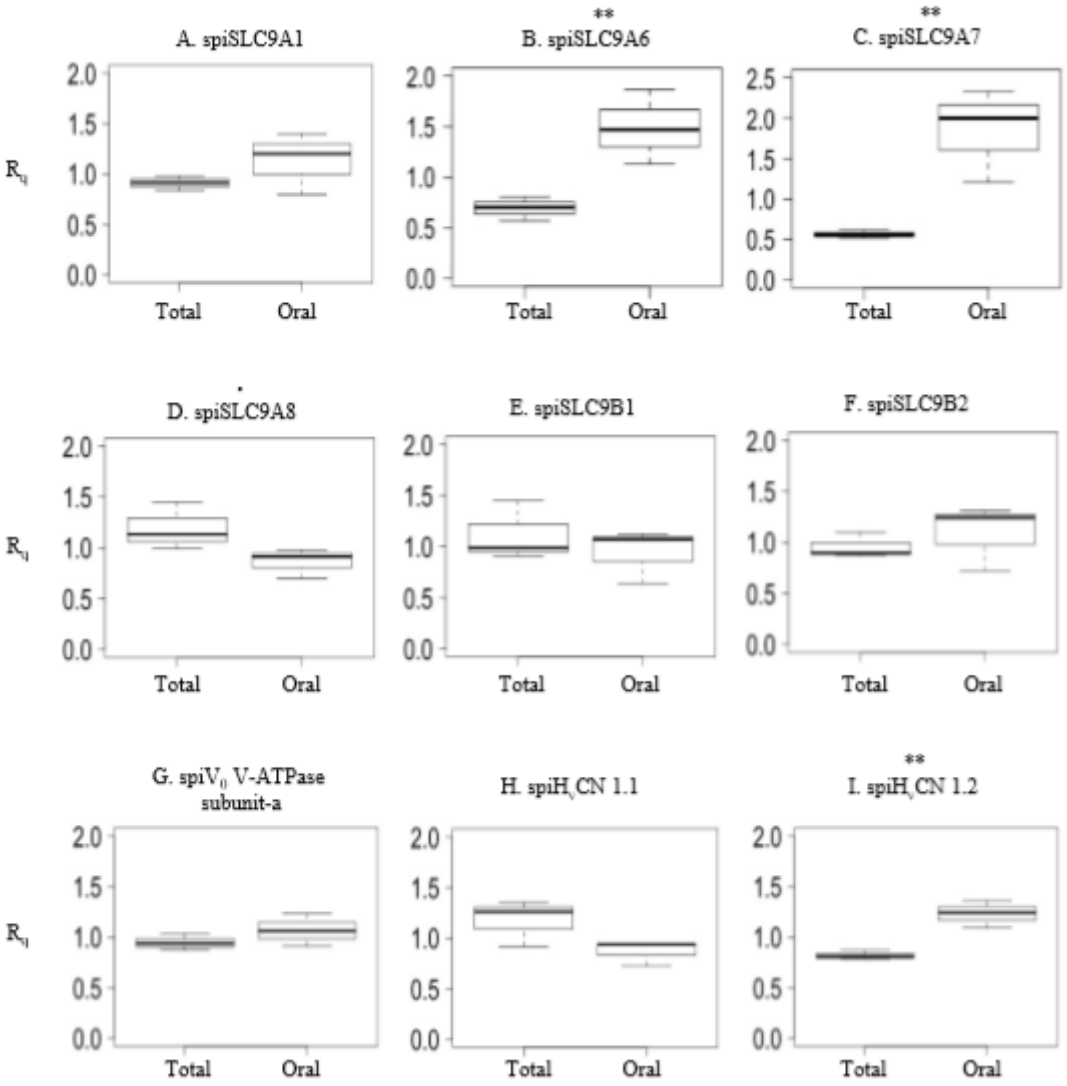

Figure 6

Relative mRNA quantification (Rq) of SLC9s, V0 V-ATPase subunit-a and HvCNs measured in total (total colony) and oral (oral fraction) fractions. Box and whisker plots show the first, second (median) and the third quartile (horizontal lines of the boxes); and respective whiskers (vertical lines spanning to the lowest and highest data point of all data, including outliers). Replicate numbers (n=3) represent separate coral samples. Asterisks and points indicate statistical difference (• 0.11≤p-value≤0.10 and ** p-value<0.05).

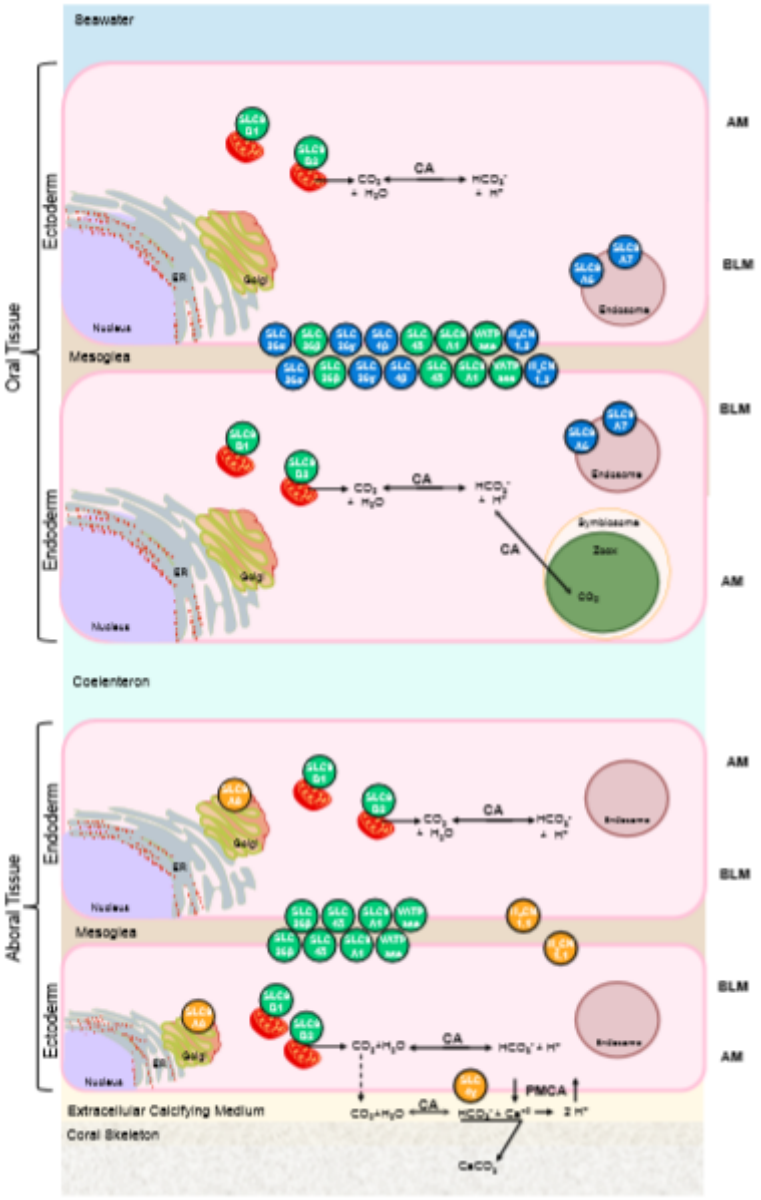

Figure 7

Model of acid-base transporters involved in intracellular pH regulation, expressed on the apical (AM) and basolateral (BLM) membrane of coral cells, throughout the tissue layers. The role of other ion channels and transporters, involved in other cellular processes, are not considered here. The model summarizes the major groups of bicarbonate (SLC4 and SLC26 transporters) and H+ transporters (SLC9, V-ATPase and HvCN) that have been identified and functionally characterized by Zoccola et al. 2015 and in the present study, respectively. In both studies, the tissue distribution of the transporters is assumed based on the results obtained by performing real-time PCR on the coral oral fraction and the total colony. Transporters that are more expressed in the oral fraction (oral specific) are coloured in blue, those that are more expressed in the total colony (aboral specific) are coloured in orange and those that are expressed at the same levels in both fractions (ubiquitous) are coloured in green. Other enzymes (CA=carbonic anhydrase) and transporters (PMCA=Ca+2 ATPase) involved in the H+ flux balance are represented in bold letters.

Supplementary Files

This is a list of supplementary files associated with this preprint. Click to download.

- AdditionalFile1.pdf
- AdditionalFile2.pdf
- AdditionalFile3.pdf
- AdditionalFile4.pdf
- AdditionalFile5.pdf
- AdditionalFile6.pdf
- AdditionalFile7.pdf
- AdditionalFile8.pdf
- AdditionalFile9.pdf
- AdditionalFile10.pdf
- AdditionalFile11.pdf
- AdditionalFile12.pdf